

Role of a highly conserved YPITP motif in 2-oxoacid:ferredoxin oxidoreductase

Heterologous expression of the gene from *Sulfolobus* sp. strain 7, and characterization of the recombinant and variant enzymes

Eriko Fukuda¹, Hiroyasu Kino¹, Hiroshi Matsuzawa² and Takayoshi Wakagi¹

¹Department of Biotechnology, The University of Tokyo, Japan; ²Department of Bioscience and Biotechnology, Aomori University, Kohbata, Japan

2-Oxoacid:ferredoxin oxidoreductase from *Sulfolobus* sp. strain 7, an aerobic and thermoacidophilic crenarchaeon, catalyses the coenzyme A-dependent oxidative decarboxylation of pyruvate and 2-oxoglutarate, a cognate Zn-7Fe-ferredoxin serving as an electron acceptor. It comprises two subunits, a (632 amino acids) and b (305 amino acids). To further elucidate its structure and function, we constructed a gene expression system. The wild-type recombinant enzyme was indistinguishable from the natural one in every criterion investigated. A series of variants was constructed to elucidate the role of the YPITP-motif (residues 253–257) in subunit a, which is conserved universally in the 2-oxoacid:ferredoxin oxidoreductase (OFOR) family. Single amino-acid replacements at Y253 and P257 by

other amino acids caused a drastic loss of enzyme activity. T256, the hydroxyl group of which has been proposed to be essential for binding of the 2-oxo group of the substrate in the *Desulfovibrio africanus* enzyme, was unexpectedly replaceable with Ala, the k_{cat} and K_{m} for 2-oxoglutarate being $\approx 33\%$ and $\approx 51\%$, respectively, as compared with that of the wild-type enzyme. Replacement at other positions resulted in a significant decrease in the k_{cat} of the reaction while the K_{m} for 2-oxoacid was only slightly affected. Thus, the YPITP-motif is essential for the turnover of the reaction rather than the affinity toward 2-oxoacid.

Keywords: archaea; ferredoxin; oxidoreductase; pyruvate; themophile.

2-oxoacid:ferredoxin oxidoreductase (OFOR) is a key enzyme catalysing the coenzyme A-dependent oxidative decarboxylation of 2-oxoacids, such as pyruvate and 2-oxoglutarate, found in all archaea [1–5], certain anaerobic bacteria [6–12], and amitochondrial eukarya [13–15]. In contrast to NAD, which plays a role in the widely distributed 2-oxoacid dehydrogenase complex [16], ferredoxin acts as an electron acceptor in the OFOR reaction [17,18]. According to the subunit composition, OFORs can be classified into three groups, the abcd-, ab-/a₂b₂-, and a₂-types. OFORs can be classified into four groups according to the specificity for 2-oxoacids; POR for pyruvate, VOR for 2-oxoisovalerate, IOR for indolepyruvate, and KOR for 2-oxo(α -keto)glutarate, which participate in the metabolism of amino acids with small side

chains, branched side chains, tryptophan, and glutamate, respectively.

The OFORs from archaea such as *Pyrococcus furiosus* [19], *Archaeoglobus fulgidus* [3], *Methanococcus thermoautotrophilicum* [20] as well as that from a pathogenic eubacterium, *Helicobacter pylori* [12], are composed of four different subunits, a (≈ 45 kDa), b (≈ 37 kDa), c (≈ 24 kDa), and d (≈ 13 kDa), and are thus referred to as abcd-type enzymes. Most of the enzymes of this type exhibit specificity for pyruvate. In certain organisms, the coexistence of an enzyme specific for 2-oxoisovalerate (VOR) has been reported [1,4,20]. The OFORs from *Sulfolobus* and *Halobacterium* possess two different subunits of 71 kDa and 37 kDa [5,21]. Subunit a is a homologue of a fusion of subunits c and a of an abcd-type OFOR, in that order. The *Sulfolobus* enzyme is characterized by its wide specificity for 2-oxoacids such as pyruvate and 2-oxoglutarate. Another OFOR capable of reacting with indolepyruvate has been found in *P. furiosus* [19] and *P. kodakaraensis* KOD1 [22], which are composed of hetero-oligomeric structure ab. Subunit a is a chimera of subunits a, d and b of an abcd-type OFOR, in that order.

The PORs from *Klebsiella pneumoniae* [6], *Rhodospirillum rubrum* [23], *Enterobacter agglomerans* 333 [24], *Rhodospirillum rubrum* (A. Lindblad, J. Jansson, E. Brostedt, M. Johansson, U. Hellman & S. Nordlund, unpublished data, EMBL accession no. X77515), *Anabaena variabilis* ATCC29413 [25], *Anabaena* PCC 7119 [11], *Trichomonas vaginalis* [26], and *Desulfovibrio africanus* [27] are homodimers of a 120–130-kDa subunit, which is a

Correspondence to T. Wakagi, The Department of Biotechnology, The University of Tokyo, 1-1-1, Yayoi-cho, Bunkyo-ku, Tokyo 113-8657, Japan. Tel./Fax: + 81 3 5841 5152,

E-mail: atwakag@mail.ecc.u-tokyo.ac.jp

Abbreviations: OFOR, 2-oxoacid:ferredoxin oxidoreductase; POR, pyruvate:ferredoxin oxidoreductase; KOR, 2-oxoglutarate(α -ketoglutarate):ferredoxin oxidoreductase; VOR, 2-oxoisovalerate:ferredoxin oxidoreductase; IOR, indolepyruvate:ferredoxin oxidoreductase.

Enzymes: pyruvate:ferredoxin oxidoreductase (pyruvate synthase; EC 1.2.7.1); 2-oxoglutarate:ferredoxin oxidoreductase (2-oxoglutarate synthase; EC 1.2.7.3).

(Received 23 July 2001, revised 31 August 2001, accepted 7 September 2001)

fusion of subunits a, c, d and b, in that order, referred as a-type enzymes in this paper.

The molecular construction of the three types of OFOR, as shown above, indicates that this family of enzymes should have evolved from a common ancestor, possibly of the abcd-type, through reorganization, deletion and fusion of the genes [5], which requires further study on the structure–function relationship of the enzyme. A molecular biological method for obtaining an altered enzyme by manipulating the gene encoding an OFOR comprises a powerful tool for such a study. Gene expression systems have been reported for *D. africanus* POR (homodimer) and *P. kodakaraensis* IOR (ab-type heterodimer). Incubation at high temperature is required for reconstitution of a heterologous structure, and enhancement of the activity of *P. kodakaraensis* IOR has been reported [28]. The recombinant *D. africanus* POR was highly labile under aerobic conditions. Deletion of the C-terminal extra stretch made the enzyme quite unstable [10]. So far there has been no report on site-directed mutagenesis of the catalytic centre of an OFOR.

Multiple alignment of amino-acid sequences revealed that members of the OFOR family show low homology with each other [5]. Despite the low homology, the YPITP motif is highly conserved and is characteristic of the OFOR family. The three-dimensional structure of *D. africanus* POR suggests that the Thr residue within the YPITP motif is involved in the 2-oxoacid recognition [29]. Therefore, the role and the structure of this unique motif should be conserved in the OFOR family. In this study, an expression system for the gene encoding an ab-type OFOR from an aerobic and thermoacidophilic crenarchaeon, *Sulfolobus* sp. strain 7, was established, which produced a recombinant enzyme indistinguishable from the natural one and a series of variants containing a single amino-acid substitution in the motif. Our results suggested that the Thr residue within the

YPITP motif was not essential for either 2-oxoacid binding or enzyme activity.

EXPERIMENTAL PROCEDURES

Bacterial strain and plasmid

Sulfolobus sp. strain 7 cells were grown as described previously [30,31]. Plasmid pZE91 [5] carrying the *ofor* gene, and pAUGE [32] carrying the *Escherichia coli* groESL and tRNA^{Arg} genes were prepared as described previously. *E. coli* strain JM109 {*recA1*, Δ (*lac-proAB*), *endA1*, *gyrA96*, *thi-1*, *hadR17*, *relA 1*, *supE 44* [F'*tra* Δ 36, *proAB*⁺, *lacIqZ* Δ M15]}, and *E. coli* strain BL21(DE3) {F⁻, *ompT* [*lon*]*hdsSB* (rB⁻ mB⁻); an *E. coli* B strain containing DE3} were used for gene manipulation. Restriction endonucleases and DNA-modifying enzymes were purchased from Nippon Gene. DNA was manipulated by means of standard procedures [33,34].

Construction of an expression plasmid

Plasmid pZE91 encoding the whole *ofor* gene [5] was used as a template for the Kunkel and PCR reactions. As the genes encoding subunits a and b overlapped by 26 bases, they were separately and/or tandemly re-arranged and ligated to an expression vector, pET17b. The gene encoding subunit-a of OFOR (*oforA*) was obtained by the Kunkel method [35] using pZE91 as a template and was subsequently cloned into the expression vector pET-17b. For the Kunkel method, two primers were designed as shown in Table 1 to replace the initiation ATG and the position after the termination TGA with an *NdeI* and a *XhoI* site, respectively.

The Kunkel method was performed using MUTA-GENE (Bio-Rad). Kunkel-AN contained an engineered *NdeI* site

Table 1. Primers used for PCR and mutagenesis. Restriction enzyme recognition sites are shown in italics.

Primer	Sequence
For expression	
Kunkel-AN	5'-CCAAC TAAGTCTCATATGTGTCAATATTCT-3'
Kunkel-AC	5'-ATCTACTCCAAGCTCGAGTATCGCTTGTTG-3'
Kunkel-BN	5'-TGTAATGCCGCCATATGACACCACCCCTCT-3'
Kunkel-BC	5'-AAAAGTTAAATTATCTCGAGTAAAATTAGTCTAC-3'
QuikChange-BN	5'-GGACCAACGCTGAGCGAGATCTCG-3'
QuikChange-BC	5'-GTTGAGATCCAGTTCGATGTA-3'
For mutation (One of the complementary chains is shown)	
Y253W	5'-CAATCATATTGGCCGATAACGCCGGCTCAGATG-3'
Y253A	5'-CAATCATATGCTCCGATAACGCCGGCTCAGATG-3'
Y253F	5'-CAATCATATTTCCGATAACGCCGGCTCAGATG-3'
P254G	5'-GATTTCAATCATATTATGGGATAACGCCGGCTCAGATG-3'
I255L	5'-CATATTATCCGCTAACGCCGGCTCAGATG-3'
I255V	5'-CAATCATATTATCCGATAACGCCGGCTCAGATG-3'
I255M	5'-CAATCATATTATCCGATGACGCCGGCTCAGATG-3'
I255S	5'-CATATTATCCGAGTACGCCGGCTCAGATG-3'
T256S	5'-GATTTCAATCATATTATCCGATATCGCCGGCTCAGATG-3'
T256A	5'-GATTTCAATCATATTATCCGATAGCGCCGGCTCAGATG-3'
T256V	5'-CAATCATATTATCCGATAGTCCGGCTCAGATG-3'
P257G	5'-CATATTATCCGATAACCGGTGCCTCAGATGAAAGTG-3'
P257A	5'-CCGATAACTGCAGCTAGCGATGAAAGTG-3'
P257V	5'-CCGATAACTGTAGCTAGCGATGAAAGTG-3'

and Kunkel-AC had an engineered *XhoI* site. The resulting 1.9-kb *oforA* gene was subcloned into *NdeI*–*XhoI* digested pET-17b. *OforA* was then sequenced to ensure that no mutations were present in the gene. The sequence was confirmed by analysing the DNA by the dideoxy chain-termination method with an Applied Biosystems Model 373A DNA sequencer (PerkinElmer). The resulting plasmid was named pOFORA.

The expression plasmid pOFORB was constructed in the same way. Primers Kunkel-BN and Kunkel-BC were designed to replace the initiation ATG and the position immediately after the termination TAA with an *NdeI* and a *XhoI* site, respectively by using pZE91 as a template. Kunkel-BN contained an engineered *NdeI* site and Kunkel-BC contained an engineered *XhoI* site. The resulting 0.9-kb *oforB* gene was subcloned into the *NdeI* and *XhoI* sites of vector pET-17b. After sequencing the inserted *oforB* fragment, the resulting plasmid was named pOFORB.

The expression plasmid pOFORAB was constructed by PCR using pOFORB as a template and subsequent cloning of this gene into pOFORA. For the PCR amplification of the *oforB* gene, two primers were designed as shown in Table 1. QuickChange-BN contained an engineered *EspI* site and QuickChange-BC had a completely complementary sequence to the pET-17b vector. The PCR amplification was performed with *Ex-taq* DNA polymerase and an Astec Program Temperature Control System PC700 programmed for 30 cycles; each cycle consisted of denaturation at 96 °C for 0.5 min, annealing at 55 °C for 1 min, and extension at 72 °C for 2 min. The resulting 0.9-kb *oforB* gene was subcloned into the *EspI* and *StyI* sites of the plasmid pOFORA. The inserted *oforB* DNA was then sequenced and the resulting plasmid was named pOFORAB.

OFOR variants were constructed by means of a 'QuickChange' site-directed mutagenesis method (Stratagene) according to the protocol recommended by the manufacturer with slight modification. For the PCR amplification of the gene from the mutation site to the end of the *oforB* strand, pOFORA was used as a template and two primers, each primer for mutations and QuickChange-BC, were used. For the PCR amplification of the gene from the initiation codon of *oforA* strand, pOFORA was used as a template, and two primers, the complementary chains of each primer for mutations and QuickChange-BN, were used. The resulting 0.86-kb and 1.3-kb fragments containing a mutation site were subcloned into the *EspI* and *StyI* sites of the pET-17b to construct pOFORAvAr. Then pOFORAvAr was digested with *HpaI*, and the resulting small fragment including a mutation site was ligated into the wild-type expression vector pOFORAB the corresponding sequence of which had been deleted. The resulting plasmid pOFORABvAr was then sequenced to certify the mutation and the resulting plasmid was named pOFORABvAr.

Production of recombinant proteins

Cells harbouring both plasmid pGroELS-AUGE and the expression plasmid for the *ofor* gene were grown in Luria–Bertani medium containing 0.1 mM FeCl₂, 25 µg·mL⁻¹ kanamycin and 100 µg·mL⁻¹ ampicillin at 36 °C, and induced by the addition of 0.1 mM isopropyl thio-β-D-galactoside until *D*₆₀₀ reached 1.0. The induced cell suspension was vigorously shaken in a Sakaguchi flask for

12 h at 25 °C. The cells were collected by centrifugation and stored frozen at –80 °C until use.

Purification of the protein

The frozen *E. coli* cells (10 g wet weight) were thawed and suspended in 50 mL of 10 mM Tris/HCl, pH 8.6, containing 0.1 mM PhCH₂SO₂F, and then disrupted by sonication. The suspension was heated at either 60 or 80 °C for 10 min, and the resulting aggregate was removed by centrifugation at 5000 g for 30 min. The supernatant obtained was defined as cell-free extract and was applied to a DEAE–Sephacel (Pharmacia) column (2 × 20 cm) pre-equilibrated with 10 mM Tris/HCl pH 8.6 (buffer I). Proteins were eluted from the column with a linear gradient of 0–0.4 M NaCl in buffer I (500 mL total). The active fractions were concentrated and applied to a Superdex 200 HR 10/30 (Pharmacia) column equilibrated with 0.1 M NaCl in buffer I. The resulting active fraction was collected and applied to a MonoQ (Pharmacia) column equilibrated with buffer I. Proteins were eluted from the column with a linear gradient of 0–0.4 M NaCl in buffer I (30 mL total). The enzyme thus prepared was used in the following experiments as the 'purified enzyme'. The natural OFOR was purified as described previously [5]. The OFOR variants were purified by the same procedure as for the wild-type recombinant OFOR. All of the purification procedures were performed under aerobic conditions.

Analytical procedures

Protein concentrations were determined by the BCA assay method (Pierce Chemical Co.) using BSA as the standard. The molecular mass of subunits a and b was determined by SDS/PAGE using 12.0% (w/v) polyacrylamide.

SDS/PAGE [36] was carried out on 12% gels after treating the proteins with 2% SDS in the presence of 2% 2-mercaptoethanol at 100 °C for 10 min, and the proteins were visualized by Coomassie brilliant blue staining.

Enzyme activity of OFOR was routinely assayed by monitoring the pyruvate-dependent reduction of methyl viologen at 80 °C in a 1.5-mL quartz cuvette containing N₂ as the gas phase. The standard assay mixture (0.5 mL) comprised 50 mM sodium phosphate pH 7.5, 10 mM sodium pyruvate, 0.25 mM CoA and 2 mM methyl viologen. For the assaying of OFOR, pyruvate was replaced with 2-oxoglutarate. To reconstitute active OFOR, 20 µL *E. coli* cell-free extracts containing subunit a and 20 µL *E. coli* cell-free extracts containing subunit b were mixed. The mixture was incubated over the temperature range 37–70 °C and the incubation time was varied over the range 5–30 min. For measurement of OFOR activity the standard assay mixture was used. For determination of the *K*_m and *k*_{cat} values for 2-oxoacids the concentration of each 2-oxoacid was varied from 0.05 to 1.5 mM; for determination of the *K*_m value for CoA the concentration of CoA ranged from 1.0 to 50 µM; the enzyme activities were measured. The rate of methyl viologen reduction was determined by following the absorbance at 578 nm ($\epsilon_{578} = 9.8 \text{ mM}^{-1}\cdot\text{cm}^{-1}$). One unit of activity is defined as 2 µmol methyl viologen reduced per min with a 2-oxoacid. The *k*_{cat} and *K*_m values were calculated by using the

Lineweaver–Burk equation measuring the activity with various concentrations of pyruvate or 2-oxoglutarate.

Mg and Fe contents were determined by inductivity-coupled plasma atomic emission spectroscopy (ICP) (SPS-1200 VR, Seiko Instruments, Chiba, Japan) using 2 mL sample solution and standard solutions of Mg and Fe (Wako Chemical Co.).

The thermostability of the natural, recombinant and variants was investigated by measuring the remaining activity at 80 °C after incubation at various temperatures for 30 min. The OFOR activity without any incubation was defined as 100% and the remaining activity after incubation was indicated by the percentage. T_m was defined as the temperature at which the activity remaining was 50%.

RESULTS

Expression of *oforA*, *oforB* and *oforAB*

The cell-free extract of recombinant *E. coli* cells carrying pOFORA gave a faint but distinct 71-kDa band corresponding to subunit a on SDS/PAGE, when pAUGE was co-expressed (data not shown). Remarkable production of subunit b was found in the extract of the cells with pOFORB and pAUGE (data not shown). These results indicate that subunit a and subunit b were soluble. The cell-free extract ($\approx 2\text{--}3\text{ mg protein}\cdot\text{mL}^{-1}$) from *E. coli* cells harboring either pOFORA or pOFORB, with or without pAUGE, was incubated for 20 min at various temperatures and then the enzyme activity was measured at 70 °C using 40 μL of each extract. No OFOR activity was detected. Subsequently, cell-free extracts of *E. coli* harbouring pOFORA and pOFORB were prepared separately as above, mixed and incubated at various temperatures to reconstruct OFOR *in vitro*. The incubation temperature ranged from 37 to 70 °C and the incubation time ranged from 5 to 30 min. The enzyme activity was measured using 40 μL of an extract mixture at various temperatures. However, very little activity ($\approx 1\%$ of the wild-type OFOR) was detected in the combined crude extract with or without heat treatment. In contrast, the extract obtained from *E. coli* cells harbouring pOFORAB showed significant activity, implying that *oforA* and *oforB* need to be translated in the same cell to constitute an active oligomer complex. These two subunits may require each

other to fold properly. OFOR activity did not vary according to heat treatment. A cell-free extract of *E. coli* cells without plasmid showed no activity.

Purification and characterization of recombinant OFOR

OFOR was purified to electrophoretic homogeneity from the cytosol fraction of *E. coli* BL21 (DE3) cells harbouring pOFORAB as described in Experimental procedures. Figure 1 shows that the heat treatment step is effective for purification. The recombinant OFOR was characterized and compared with OFOR purified from *Sulfolobus* sp. strain 7 cells (designated as 'natural OFOR'). The recombinant enzyme exhibited k_{cat} values of 48 and 17 s^{-1} with pyruvate and 2-oxoglutarate, respectively. For comparison, the k_{cat} values of natural OFOR were 51 s^{-1} with pyruvate and 19 s^{-1} with 2-oxoglutarate. As shown in Table 2, the recombinant and natural OFORs exhibit almost the same catalytic properties, optimum temperature (Fig. 1C), and optimum pH (Fig. 1B).

The results imply that a reliable system for the production of a highly stable recombinant OFOR, indistinguishable from the natural one, has been established for the first time. Recombinant IOR from *P. kodakaraensis* has been reported [28]. Incubation of the cell-free extract of the recombinant *E. coli* was required for activation of the enzyme. This was attributed to heat-induced rearrangement of the quaternary structure. In contrast, the activity of the recombinant OFOR from *Sulfolobus* was independent of thermal treatment. Heat treatment of the extract from recombinant *E. coli* did not increase the total activity of the enzyme. It should also be pointed out that the 'activated IOR' purified from the recombinant *E. coli* carrying the *P. kodakaraensis ifor* gene showed a k_{cat} of $\approx 0.68\text{ s}^{-1}$ at optimum temperature (70 °C), which is much lower than that reported for *P. furiosus* IOR (114 s^{-1} at 80 °C) [19]. Another example is the POR gene expression system of *D. africanus* [10]. The recombinant POR showed similar characteristics to those of the natural enzyme, and completely lost its activity within 1 week due to its high sensitivity to oxygen. The C-terminal extension, specifically found in the enzyme, is related to this stability, as shown by the deletion experiment.

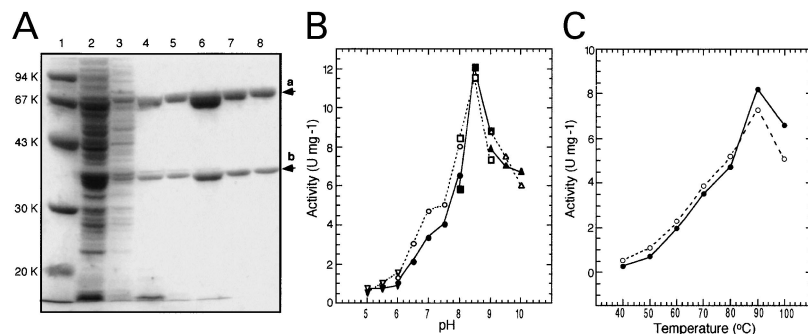


Fig. 1. Comparison of the natural and wild-type recombinant 2-oxoacid:ferredoxin oxidoreductases from *Sulfolobus* sp. strain 7.

(A) SDS/PAGE analysis of the recombinant OFOR. Lane 1, molecular mass markers; lane 2, cell-free extract; lane 3, heat-treated precipitate; lane 4, heat-treated supernatant; lane 5, DEAE–Sephacel; lane 6, Superdex 200; lane 7, MonoQ; lane 8, natural OFOR. (B) Effects of pH on the activities of the natural (broken line) and wild-type recombinant (solid line) OFORs. The buffers used were 20 mM acetate/NaOH for pH 5.0–6.0 (∇ , \blacktriangledown), 20 mM sodium phosphate for pH 6.0–8.0 (\circ , \bullet), 20 mM borate/NaOH for pH 8.0–9.0 (\square , \blacksquare), and 20 mM Ches cyclohexylaminoethane sulfonic acid/NaOH for pH 9.0–10.0 (\triangle , \blacktriangle). (C) Temperature dependence of the activities of the natural (broken line) and wild-type recombinant (solid line) OFORs.

Table 2. Characterization of the natural and recombinant OFORs.

	Natural	Recombinant
Molecular mass (gel filtration)	105 kDa	105 kDa
Subunit (SDS/PAGE)	a, 71 kDa b, 34 kDa	a, 71 kDa b, 34 kDa
Cofactor/substrate		
[4Fe-4S] cluster ^a	1 mol·mol ⁻¹	1 mol·mol ⁻¹
Thiamine-diphosphate	0.6 mol·mol ⁻¹ ^b	
Magnesium ^c	1.4 mol·mol ⁻¹	1.9 mol·mol ⁻¹
Pyruvate		
k_{cat}	51·s ⁻¹	48·s ⁻¹
K_m	0.25 mM	0.33 mM
2-oxoglutarate		
k_{cat}	19·s ⁻¹	17·s ⁻¹
K_m	0.87 mM	0.72 mM
Temperature optimum	90 °C	90 °C
pH optimum ^d	8.5	8.5
Arrhenius activation energy ^e	39 kJ·mol ⁻¹	42 kJ·mol ⁻¹
Stability ^f	60%	58%

^a Deduced from the EPR spectra and the iron content (2.6 and 3.1 mol·mol⁻¹ protein for the natural and recombinant enzymes, respectively) determined by ICP spectroscopy. ^b Previously reported [5]. ^c ICP spectroscopy. ^d pH adjusted at 25 °C, see Fig. 1B. ^e Calculated from Fig. 1C. ^f Percentage ratio of remaining activity after incubation at 80 °C and 25 °C for 30min in 20 mM sodium phosphate pH 7.2. The enzyme concentrations were 0.1 mg·mL⁻¹.

The role of the YPITP motif of OFOR

Because an OFOR gene expression system was established as above, mutated OFOR from *Sulfolobus* became available. There are several highly conserved motifs in the OFOR family, including the thiamin pyrophosphate binding site [37], adenine recognition loop for the CoA binding site

[38,39], the [4Fe-4S] cluster binding site and the YPITP motif. The YPITP motif is found in subunit a (positions 253–257) in *Sulfolobus* sp. strain 7. Despite the strict conservation of the five amino-acid sequence, the function of the YPITP motif is unknown. To determine the role of this motif we introduced point mutations into the motif and characterized the OFOR variants. *E. coli* BL21 (DE3) cells harbouring plasmids for expression of OFOR variants were cultured and disrupted by sonication. Then the cell extracts were heat-treated and supernatants were recovered by centrifugation. All of the OFOR variants were well expressed, as shown in Fig. 2A, and were purified to electrophoretic homogeneity electrophoretic homogeneity by the method described in Experimental procedures (Fig. 2B). **Table 3 summarizes the OFOR activities of the YPITP variants.** The Y253W, Y253A, P257G, P257A and P257V showed no enzyme activity at either 50 or 80 °C. On the other hand, the Y253F, P254G, I255L, I255V, I255M, I255S, T256A, T256V and T256S exhibited OFOR activity, although the k_{cat} values with pyruvate and 2-oxoglutarate were lower than those for the wild-type OFOR by \approx 10% and \approx 50%, respectively.

Affinity to CoA

To examine the possibility that the YPITP motif plays some role in CoA binding, kinetic parameters were determined using the Y253F. The K_m values for CoA were 17 and 23 μ M for the wild-type and Y253F enzymes, respectively. The k_{cat} values of the variants did not increase even when an extra 2.5 mM CoA was added to the reaction mixture. Therefore, the motif is unlikely to bind to CoA.

Thermostability of OFOR variants

We examined the thermostability of the OFOR variants that showed some activity. The remaining activity after

Table 3. Kinetic parameters of the OFOR variants.

	Substrate						
	Pyruvate			2-oxoglutarate			
	k_{cat} (s ⁻¹)	K_m (mM)	k_{cat}/K_m (s ⁻¹ ·mM ⁻¹)	k_{cat} (s ⁻¹)	K_m (mM)	k_{cat}/K_m (s ⁻¹ ·mM ⁻¹)	
Natural	51	0.28	182	19	0.85	22	
Recombinant	48	0.33	146	17	0.72	23	
Y253W	0		0	0		0	
Y253A	0		0	0		0	
Y253F	2.2	0.31	7.2	5.3	1.5	3.6	
P254G	3.6	0.17	21	5.2	1.2	4.3	
I255L	5.7	0.28	20	5.1	1.1	4.6	
I255S	3.2	0.13	25	7.4	0.89	8.3	
I255V	6.0	0.25	24	1.7	3.3	0.52	
I255M	7.9	0.19	41	10	1.3	7.7	
T256S	4.1	0.11	38	7.4	2.1	3.4	
T256A	4.3	0.14	31	5.5	0.37	15	
T256V	4.6	0.17	28	6.7	0.33	20	
P257G	0		0	0		0	
P257A	0		0	0		0	
P257V	0		0	0		0	

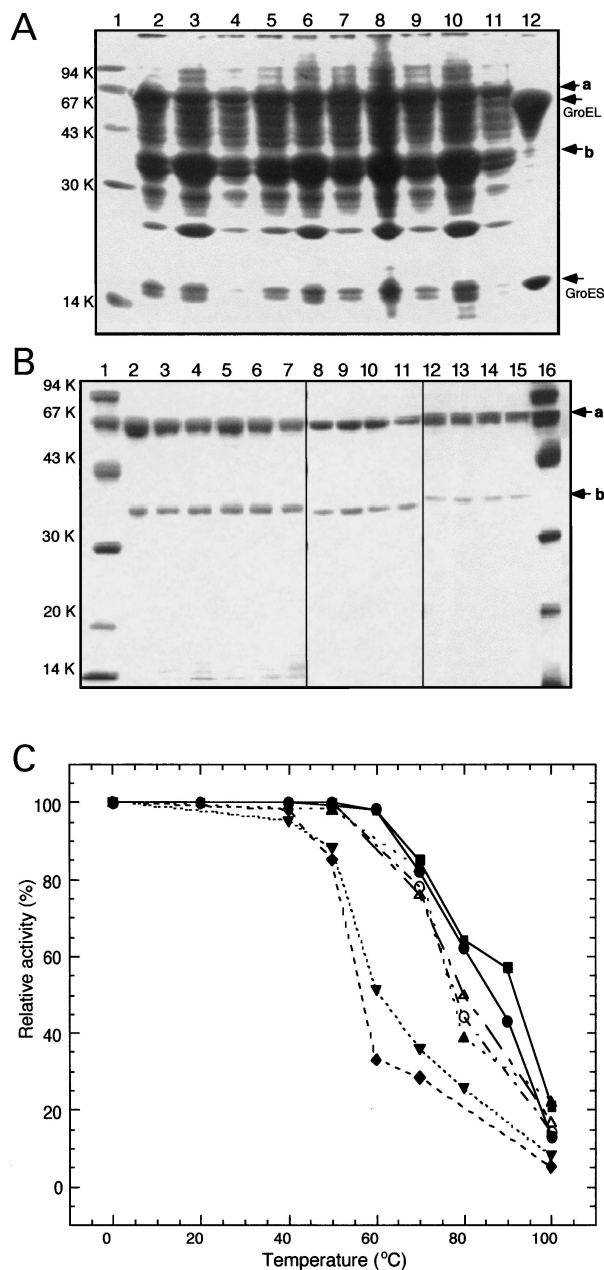


Fig. 2. Comparison of variants of the 2-oxoacid:ferredoxin oxidoreductases from *Sulfolobus* sp. strain 7. (A) SDS/PAGE analysis of *E. coli* cell extracts harbouring plasmids encoding various OFOR variants. Lane 1, markers; lane 2, wild-type recombinant OFOR; lane 3, Y253W; lane 4, Y253A; lane 5, P254G; lane 6, I255L; lane 7, I255S; lane 8, T256S; lane 9, T256A; lane 10, P257G; lane 11, P257A; lane 12, P257V. (B) SDS/PAGE of the purified OFOR variants. Lanes 1 and 16, markers; lane 2, wild-type recombinant OFOR; lane 3, P254G; lane 4, I255L; lane 5, I255S; lane 6, T256S; lane 7, T256A; lane 8, natural OFOR; lane 9, wild-type recombinant OFOR; lane 10, Y253F; lane 11, I255M; lane 12, I255V; lane 13, Y253W; lane 14, T256V; lane 15, P257G. Protein amounts used were about 6–8 μ g for lanes 2–7, 4–5 μ g for lanes 8–11, and 2–3 μ g for lanes 12–15. (C) Thermostability of the natural OFOR (●), wild-type recombinant OFOR (■), P254G (◆), I255L (▲), I255S (▼), T256S (△), and T256A (○). The enzymes were incubated at various temperatures for 30 min. Aliquots were withdrawn and assayed for the remaining activity at 80 °C.

incubation for 30 min at various temperatures was determined. The results are shown in Fig. 2C. All of the OFOR variants exhibited almost the same thermal stability as the natural OFOR and recombinant wild-type OFOR except for P254G and I255S. The T_m values of P254G and I255S were ≈ 20 °C lower than those of the other enzymes, which may be explained partly by the increase in the flexibility of the motif, as discussed later.

DISCUSSION

Because OFORs from anaerobes are unstable under aerobic conditions, the preparation of the enzymes from these organisms must be performed under strictly anoxic conditions [27]. Recombinant OFORs described previously have serious problems with both stability [10] and activity [28]. In contrast, *Sulfolobus* OFOR is quite stable under aerobic conditions and is thus handled easily. This is the first report of the establishment of a gene expression system that produces a recombinant OFOR indistinguishable from the natural one (Table 2).

We used the gene expression system to elucidate the functional role of the YPITP motif. We introduced a single point-mutation into the motif and characterized the OFOR variants (Table 3). Single amino-acid replacements at Y253 and P257 caused a drastic loss of enzyme activity. Replacement at other positions resulted in a significant decrease in the k_{cat} of the reaction while the K_m for 2-oxoacid was affected only slightly. For an unknown reason, most of the mutated enzymes showed lower k_{cat} values for pyruvate than that for 2-oxoglutarate.

Y253F showed $\approx 4\%$ of the wild-type enzyme activity toward pyruvate, but Y253W and Y253A lost the activity completely. This indicates that the aromatic ring, but not the indole ring, at position 253 is required for enzyme activity, and that the phenolic hydroxyl group enhances the reaction rate. In the OFOR family a few exceptions have been reported in which Y253 is replaced by Phe, such as the POR from *Pyrococcus furiosus* [1]. This is consistent with our results, and the aromatic ring at position 253 may be accompanied by a hydroxyl group from another residue.

Although Y253F lost most of the OFOR activity, its K_m value for CoA was 23 μ M, similar to that of the wild-type enzyme. This, together with the similar K_m for pyruvate (0.31 mM) to that of the wild-type (0.28 mM) suggests that the residue has little relation to binding of the substrate or the cofactor.

The P254 and I255 variants exhibited OFOR activity although their k_{cat} values were lower than that of the wild-type enzyme. Of the four variants based on I255, I255M showed the highest activity for both pyruvate and 2-oxoglutarate. This is consistent with the fact that the motif is modified to YPMTTP in *H. salinarum* POR [40]. The catalytic efficiency of these variants are lower than that of the wild-type, due to their low k_{cat} values.

Among the five residues, only Thr was suggested to interact directly with the carbonyl oxygen of the substrate, based on the results of X-ray crystallography of *D. africanus* POR complexed with pyruvate at 3-Å resolution [29]. But contrary to the expectation that the Thr residue must be essential for substrate recognition, the three T256 variants exhibit OFOR activity. This indicates that not only the hydroxyl group of Thr but also some other

atoms recognize the substrate. The genes encoding putative OFORs from *Sulfolobus solfataricus* P1 and *Sulfolobus solfataricus* P2 revealed that the Thr residues were replaced by Arg in these species, which also suggests that the hydroxyl group of Thr is not essential for substrate recognition (Y. Nishizawa, E. Fukuda and T. Wakagi, unpublished observation).

The P257 variants exhibited no OFOR activity, which indicates that P257 is essential. The structure around the YPITP motif of *D. africanus* POR revealed that the last Pro of the motif (P257 for *Sulfolobus* OFOR) was in a special *cis* conformation. A *cis* conformation is usually not allowed for residues other than Pro, so any mutation of the P257 may affect the main chain fold of YPITP motif and thereby perturb its structural integrity.

Thus, single amino-acid replacement in the YPITP-motif resulted in a significant decrease in the turnover of the reaction. In contrast, the role of each residue in 2-oxoacid binding is not evident; some of the variant enzymes show lower K_m values than the wild-type.

Investigation of the thermostability of the OFOR variants indicated clearly that the T_m values of P254G and I255S were ≈ 20 °C lower than those of the wild-type OFOR and other OFOR variants (Fig. 2C). The most plausible explanation for this result is that, with the substitution of a proline by a glycine, the increase in the flexibility and the loose conformation cause the lower thermostability of P254G. As deduced from the three-dimensional structure of the POR from *D. africanus*, the I255 residue seems to be deeply buried in the molecule [29]. It is said that the substitution of a hydrophobic amino acid in a hydrophobic environment to a hydrophilic amino acid is energetically unfavourable. Therefore, replacement of an Ile residue at position 255 by a Ser should cause destabilization of I255S.

All YPITP variants that exhibit enzyme activity show significantly lower k_{cat} values than that of the wild-type enzyme (6–20 times lower), but the K_m values are only different by ≈ 0.5 –2 times. Therefore a valid conclusion is that that the conserved YPITP motif is concerned mainly with the turnover of the reaction. One possibility is that the YPITP motif is flexible and that its mobility is important for efficient catalysis of the reaction. Variants in to the YPITP motif should lack such flexibility and therefore exhibit lower activity.

ACKNOWLEDGEMENTS

The authors thank K. Okamoto (deceased) for the amino-acid sequence analyses, S. Fushinobu for the helpful discussion, and H. Imamura for the development of the expression vectors.

REFERENCES

- Kletzin, A. & Adams, M.W.W. (1996) Molecular and phylogenetic characterization of pyruvate and 2-ketoisovalerate ferredoxin oxidoreductases from *Pyrococcus furiosus* and pyruvate ferredoxin oxidoreductase from *Thermotoga maritima*. *J. Bacteriol.* **178**, 248–257.
- Bult, C.J., White, O., Olsen, G.J., Zhou, L., Fleischmann, R.D., Sutton, G.G., Blake, J.A., FitzGerald, L.M., Clayton, R.A., Gocayne, J.D., Kerlavage, A.R., Dougherty, B.A., Tomb, J.F., Adams, M.D., Reich, C.I., Overbeek, R., Kirkness, E.F., Weinstock, K.G., Merrick, J.M., Glodek, A., Scott, J.L., Geoghagen, N.S.M. & Venter, J.C. (1996) Complete genome sequence of the methanogenic archaeon, *Methanococcus jannaschii*. *Science* **273**, 1058–1073.
- Kunow, J., Linder, D. & Thauer, R.K. (1995) Pyruvate: ferredoxin oxidoreductase from the sulfate-reducing *Archaeoglobus fulgidus*: molecular composition, catalytic properties, and sequence alignment. *Arch. Microbiol.* **163**, 21–28.
- Heider, J., Mai, X. & Adams, M.W.W. (1996) Characterization of 2-ketoisovalerate ferredoxin oxidoreductase, a new and reversible coenzyme A-dependent enzyme involved in peptide fermentation by hyperthermophilic archaea. *J. Bacteriol.* **178**, 780–787.
- Zhang, Q., Iwasaki, T., Wakagi, T. & Oshima, T. (1996) 2-Oxoacid: ferredoxin oxidoreductase from the thermoacidophilic archaeon, *Sulfolobus* sp. strain 7. *J. Biochem.* **120**, 587–599.
- Arnold, W., Rump, A., Klipp, W., Priefer, U.B. & Pühler, A. (1988) Nucleotide sequence of a 24,206-base-pair DNA fragment carrying the entire nitrogen fixation gene cluster of *Klebsiella pneumoniae*. *J. Mol. Biol.* **203**, 715–738.
- Lindblad, A., Jansson, J., Brostedt, E., Johansson, M., Hellman, U. & Nordlund, S. (1996) Identification and sequence of a *nifJ*-like gene in *Rhodospirillum rubrum*: partial characterization of a mutant unaffected in nitrogen fixation. *Mol. Microbiol.* **20**, 559–568.
- Krutzer, R., Dayananda, S. & Klingmuller, W. (1989) Identification and characterization of the *nifH* and *nifJ* promoter regions located on the *nif*-plasmid pEA3 of *Enterobacter agglomerans* 333. *Gene* **78**, 101–109.
- Blamey, J.M. & Adams, M.W.W. (1994) Characterization of an ancestral type of pyruvate:ferredoxin oxidoreductase from the hyper thermophilic bacterium *Thermotoga maritima*. *Biochemistry* **33**, 1000–1007.
- Pieulle, L., Magro, V. & Hatchikian, E.C. (1997) Isolation and analysis of the gene encoding the pyruvate-ferredoxin oxidoreductase of *Desulfovibrio africanus*, production of the recombinant enzyme in *Escherichia coli*, and effect of carboxy-terminal deletions on its stability. *J. Bacteriol.* **179**, 5684–5692.
- Schmitz, O., Kentemich, T., Zimmer, W., Hundeshagen, B. & Bothe, H. (1993) Identification of the *nifJ* gene coding for pyruvate: ferredoxin oxidoreductase in dinitrogen-fixing cyanobacteria. *Arch. Microbiol.* **160**, 62–67.
- Hughes, N.J., Clayton, C.L., Chalk, P.A. & Kelly, D.J. (1998) *Helicobacter pylori* *porCDAB* and *oorDABC* genes encode distinct pyruvate: flavodoxin and 2-oxoglutarate: acceptor oxidoreductases which mediate electron transport to NADP. *J. Bacteriol.* **180**, 1119–1128.
- Hrdy, I. & Muller, M. (1995) Primary structure and eubacterial relationships of the pyruvate: ferredoxin oxidoreductase of the amitochondriate eukaryote, *Trichomonas vaginalis*. *J. Mol. Evol.* **41**, 388–396.
- Rodriguez, M.A., Garcia-Perez, R.M., Mendoza, L., Sanchez, T., Guillen, N. & Orozco, E. (1998) The pyruvate:ferredoxin oxidoreductase enzyme is located in the plasma membrane and in a cytoplasmic structure in *Entamoeba*. *Microb. Pathog.* **25**, 1–10.
- Townson, S.M., Upcroft, J.A. & Upcroft, P. (1996) Characterisation and purification of pyruvate:ferredoxin oxidoreductase from *Giardia duodenalis*. *Mol. Biochem. Parasitol.* **79**, 183–193.
- Koike, M. & Koike, K. (1976) Structure, assembly, and function of mammalian α -keto acid dehydrogenase complexes. *Adv. Biophys.* **9**, 187–227.
- Kerscher, L. & Oesterheld, D. (1982) Pyruvate: ferredoxin oxidoreductase – new findings on an ancient enzyme. *Trends. Biochem. Sci.* **7**, 371–374.
- Danson, M.J. (1989) Central metabolism of the archaeobacterium: an overview. *Can. J. Microbiol.* **35**, 58–64.
- Mai, X. & Adams, M.W.W. (1994) Indolepyruvate ferredoxin oxidoreductase from the hyperthermophilic archaeon *Pyrococcus*

- furiosus*. A new enzyme involved in pepride fermentation. *J. Biol. Chem.* **269**, 16726–16732.
20. Tersteegen, A., Linder, D., Thauer, R.K. & Hedderich, R. (1997) Structures and functions of four anabolic 2-oxoacid oxidoreductases in *Methanobacterium thermoautotrophicum*. *Eur. J. Biochem.* **244**, 862–868.
 21. Kerscher, L. & Oesterhelt, D. (1981) Purification and properties of two 2-oxoacid: ferredoxin oxidoreductases from *Halobacterium halobium*. *Eur. J. Biochem.* **116**, 587–594.
 22. Siddiqui, M.A., Fujiwara, S. & Imanaka, T. (1997) Indolepyruvate ferredoxin oxidoreductase from *Pyrococcus* sp. KOD1 possesses a mosaic structure showing features of various oxidoreductases. *Mol. Gen. Genet.* **254**, 433–439.
 23. Brostedt, E. & Nordlund, S. (1991) Purification and partial characterization of a pyruvate oxidoreductase from the photosynthetic bacterium *Rhodospirillum rubrum* grown under nitrogen-fixing conditions. *Biochem. J.* **279**, 155–158.
 24. Kreutzer, R., Dayananda, S. & Klingmuller, W. (1991) Cotranscription of the electron transport protein genes *nifJ* and *nifH* in *Enterobacter agglomerans* 333. *J. Bacteriol.* **173**, 3252–3256.
 25. Yakunin, A.F., Hallenbeck, P.C., Troshina, O.Y. & Gogotov, I.N. (1993) Purification and properties of a bacterial-type ferredoxin from the nitrogen-fixing cyanobacterium *Anabaena variabilis* ATCC29413. *Biochim. Biophys. Acta.* **1163**, 124–130.
 26. Williams, K., Lowe, P.N. & Leadlay, P.F. (1987) Purification and characterization of pyruvate: ferredoxin oxidoreductase from the anaerobic protozoa, *Trichomonas vaginalis*. *Biochem. J.* **246**, 529–536.
 27. Pieulle, L., Guigliarelli, B., Asso, M., Dole, F., Bernadac, A. & Hatchikian, E.C. (1995) Isolation and characterization of the pyruvate-ferredoxin oxidoreductase from the sulfate-reducing bacterium *Desulfovibrio africanus*. *Biochim. Biophys. Acta.* **1250**, 49–59.
 28. Siddiqui, M.A., Fujiwara, S., Takagi, M. & Imanaka, T. (1998) In vitro heat effect on heterooligomeric subunit assembly of thermostable indolepyruvate ferredoxin oxidoreductase. *FEBS Lett.* **434**, 372–376.
 29. Chabriere, E., Charon, M.H., Volbeda, A., Pieulle, L., Hatchikian, E.C. & Fontecilla-Camps, J.C. (1999) Crystal structures of the key anaerobic enzyme pyruvate: ferredoxin oxidoreductase, free and in complex with pyruvate. *Nat. Struct. Biol.* **6**, 182–190.
 30. Iwasaki, T., Wakagi, T., Isogai, Y., Tanaka, K., Iizuka, T. & Oshima, T. (1994) Functional and evolutionary implications of a [3Fe–4S] cluster of the dicluster-type ferredoxin from the thermoacidophilic archaeon, *Sulfolobus* sp. strain 7. *J. Biol. Chem.* **269**, 29444–29450.
 31. Amano, T., Wakagi, T. & Oshima, T. (1993) An ecto-enzyme from *Sulfolobus acidocaldarius* strain 7 which catalyzes hydrolysis of inorganic pyrophosphate, ATP, and ADP: purification and characterization. *J. Biochem. (Tokyo)* **114**, 329–333.
 32. Imamura, H., Jeon Beong-Sam, Wakagi, T. & Matsuzawa, H. (1999) High level expression of *Thermococcus litoralis* 4- α -glucanotransferase in a soluble form in *Escherichia coli* with a novel expression system involving minor arginine tRNAs and GroELS. *FEBS Lett.* **457**, 393–396.
 33. Sambrook, J., Fritsch, E.F. & Maniatis, T. (1989) *Molecular Cloning: A Laboratory Manual*, Vol. 3, 2nd edn. Cold Spring Harbor Laboratory Press, Cold Spring Harbor, New York, USA.
 34. Ausubel, F.M., Brent, R., Kingston, R.E., Moore, D.D., Seidman, J.G. & Struhl, K. (1987) *Current Protocols in Molecular Biology*. Wiley, New York, USA.
 35. Kunkel, T.A. (1985) The mutational specificity of DNA polymerase-beta during in vitro DNA synthesis. Production of frameshift, base substitution, and deletion mutations. *J. Biol. Chem.* **260**, 5787–5796.
 36. Laemmli, U.K. (1970) Cleavage of structural proteins during the assembly of the head of bacteriophage T4. *Nature* **227**, 680–685.
 37. Hawkins, C.F., Borges, A. & Perham, R.N. (1989) A common structural motif in thiamin pyrophosphate-binding enzymes. *FEBS Lett.* **255**, 77–82.
 38. Remington, S., Wiegand, G. & Huber, R. (1982) Crystallographic refinement and atomic models of two different forms of citrate synthase at 2.7 and 1.7 Å resolution. *J. Mol. Biol.* **158**, 111–152.
 39. Russell, R.J., Hough, D.W., Danson, M.J. & Taylor, G.L. (1994) The crystal structure of citrate synthase from the thermophilic archaeon, *Thermoplasma acidophilum*. *Structure.* **2**, 1157–1167.
 40. Plaga, W., Lottspeich, F. & Oesterhelt, D. (1992) Improved purification, crystallization and primary structure of pyruvate: ferredoxin oxidoreductase from *Halobacterium halobium*. *Eur. J. Biochem.* **205**, 391–397.